

Finite Element Simulation for Mechanical Behavior of Carbon/Polyphenylene Sulfide Composite Laminates

*Viet Dung Luong¹, Pham Tuong Minh Duong²

¹University of Reims Champagne-Ardenne, France

²Thai Nguyen University of technology, Vietnam

Abstract: In this paper, in addition to the experimental tests with notched specimens, based on the finite element methods, plastic models and viscoelastic - viscoplastic models, we have developed a code finite element (Cast3M) for a numerical modelling to simulate the tensile test, charge-discharge test and fatigue test for $[\pm 45]_7$ Angle-ply (AP) Carbon/Polyphenylene Sulfide (C/PPS) composites at temperature test $T = 1200$ C. On the other hand, in engineering design, over stresses at stress concentrators is very important because they are directly related to the strength of the structure, so we also simulated the overstress profiles near the hole in notched in this study. The numerical results obtained are in good agreement with the experimental results.

Keywords: Fatigue, Thermoplastic, Thermoset, Finite element, Simulation, Cast3M

Date of Submission: 30-08-2017

Date of acceptance: 13-09-2017

I. INTRODUCTION

Over the past decade, several studies have shown that metals and composite materials accumulate damage in different ways under cyclic loading. In metals, failure usually occurs after the propagation of a single macroscopic crack. In composites, failure usually occurs at places after accumulation of multiple damage modes in composite materials, such as crazing and cracking of matrix, fiber/matrix debonding, fiber fracture, transverse-ply cracking, delamination, and multidirectional cracking [1]. To describe the fatigue behavior of these materials, many plastic models and viscoelastic - viscoplastic models are established. Initially, most of these models are established for polymeric materials. The first is the simple empirical laws to predict linear viscoelastic behavior [2]. Then, these models were adjusted and extended for composite materials. A few micromechanical modelling approaches have been developed for predicting effective viscoelastic behaviors of particle reinforced composites as Maxwell, Voigt, SLS, Boltzmann, Findley, Schapery, Spectral and some other models [3-7]. Each model has different advantages and disadvantages: For the Schapery's model, many authors tried to improve to enlarge its application field. For the viscoplastic model, Schapery's viscoelastic model has been associated with simple viscoplastic formulations in order to more accurately predict the behavior of polymeric materials [8]. However, for thermoplastic-based composites, this approach has very little application. To describe the viscoplastic behavior of fiber reinforced polymer matrix composites, several phenomenological models have been developed [2,9-17], in which we can find the dependence on temperature and time of Carbon/Thermoplastic laminates at temperatures higher than T_g , several formulations are based on nonlinear isotropic and kinematic hardening.

Using finite element simulations allow avoiding numerous experimental tests and predicting possible failures during the early design stage. Based on viscoelastic - viscoplastic model [18], we have developed a code finite element (Cast3M) to simulate experiments on mechanical behavior for C/PPS composite. Besides, we also conducted the corresponding experiments to compare the results with the simulation ones.

II. MATERIALS AND EXPERIMENT

The experiments were proceed on MTS 810 servo-hydraulic testing machine at room moisture. The specimens is clamped by hydraulic jaws. A thermal chamber is embellished to carry out the temperature tests. The axial displacements are measured by an extensometer of initial length $L_0 = 60$ mm. The investigated material are $[\pm 45]_7$ AP C/PPS at temperature test $T = 120^\circ\text{C}$ and oscillation frequency is 10 Hz. The hole factor C_h represents the hole sensitivity of the laminate ultimate strength. It is defined by $C_h = \sigma_{notched}^u / \sigma_{unnotched}^u$, where $\sigma_{notched}^u = F_{notched}^u / t \cdot w$ and $\sigma_{unnotched}^u = F_{unnotched}^u / t \cdot w$ are respectively the notched and unnotched ultimate stresses, t and w are the thickness and width of the specimen respectively. The dimensions of specimen are shown in Fig. 1.

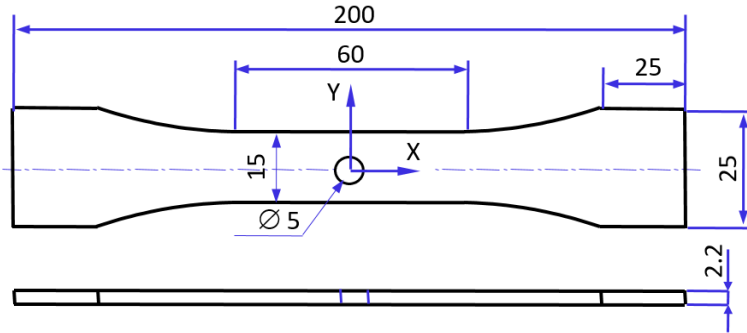


Fig. 1. Dimensions of the specimen

First, we performed the tensile tests on notched laminates to determine the mechanical behavior of material (Fig.2a). After determining stress rupture ($\sigma_{rupt} = 142$ MPa), the fatigue experiments conducted with three applied level stress are: 50% σ_{rupt} , 60% σ_{rupt} , 70% σ_{rupt} at five different times: 20%, 40%, 60%, 80%, and 100% of cycle fatigue. The behavior of AP laminates shown in Fig.2b.

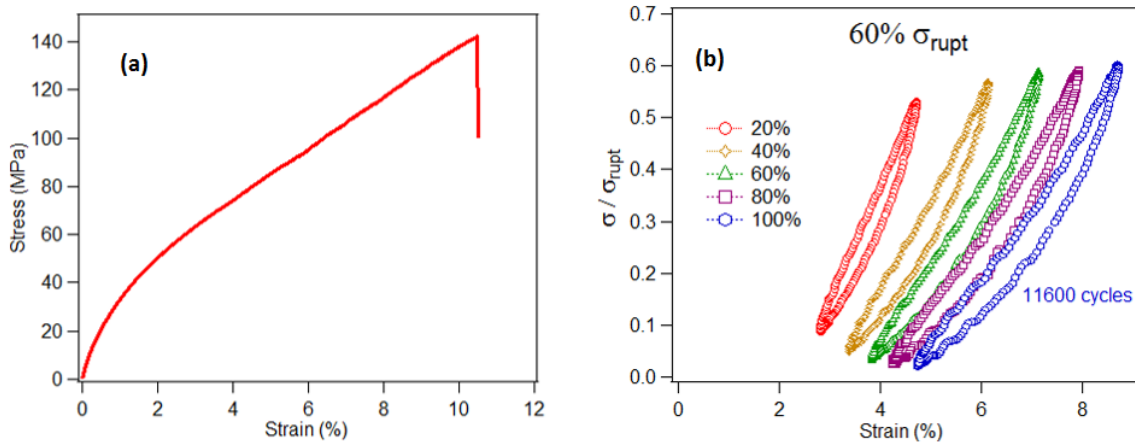


Fig. 2. Behavior of AP laminates C/PPS: (a) Tensile test, (b) Fatigue loading test

III. FINITE ELEMENT MODEL

In this study, we used the viscoelastic - viscoplastic model [18] to describe the behavior of composite laminates. The tensor of the total deformations was calculated by the hypothesis of small deformations:

$$\underline{\underline{\varepsilon}} = \underline{\underline{\varepsilon}}^e + \underline{\underline{\varepsilon}}^{ve} + \underline{\underline{\varepsilon}}^{vp} \quad (1)$$

where $\underline{\underline{\varepsilon}}^e$ is elastic deformation, $\underline{\underline{\varepsilon}}^{ve}$ is viscoelastic deformation, $\underline{\underline{\varepsilon}}^{vp}$ is viscoplastic deformation.

It should be noted that the tensors are written in direct notations: $\underline{\underline{(\cdot)}}$ represents a second order tensor and $\underline{\underline{(\cdot)}}$ represents a fourth order tensor. A superposed dot indicates the rate, a superpose -1 the inverse and a superposed T the transpose. $\underline{\underline{I}}$ and $\underline{\underline{I}}$ are the second and the fourth order identity tensors respectively. The viscoelastic spectral model lays on the decomposition of the viscoelastic strain rate $\dot{\underline{\underline{\varepsilon}}}^{ve}$ in elementary kinetics $\dot{\underline{\underline{\xi}}}_i$ ($i \in N$) associated with a relaxation spectrum according to a Gaussian distribution.

$$\dot{\underline{\underline{\varepsilon}}}^{ve} = \sum_{i=1}^{n_b} \dot{\underline{\underline{\xi}}}_i \quad (2)$$

Once the mechanisms are identified on the Gaussian distribution, we must comply with the following differential equation deriving from a thermodynamically potential [19]:

$$\dot{\underline{\underline{\xi}}}_i = \frac{1}{\tau_i} (\mu_i \underline{\underline{S}}^{ve} \underline{\underline{\sigma}} - \underline{\underline{\xi}}_i) \quad (3)$$

where $\underline{\underline{\sigma}}$ is the Cauchy stress tensor and $\underline{\underline{S}}^{ve}$ is the viscoelastic compliances tensor. In the case of a woven ply, it can be defined by:

$$\underline{\underline{S}}^{ve} = \begin{pmatrix} 0 & 0 & 0 & 0 & 0 & 0 \\ 0 & 0 & 0 & 0 & 0 & 0 \\ 0 & 0 & 0 & 0 & 0 & 0 \\ 0 & 0 & 0 & \beta_{44} / G_{12} & 0 & 0 \\ 0 & 0 & 0 & 0 & \beta_{44} / G_{12} & 0 \\ 0 & 0 & 0 & 0 & 0 & 0 \end{pmatrix} \quad (4)$$

where β_{44} is a material time-dependent parameter and G_{12} is the shear modulus. The coefficient μ_i represent the weight of each elementary mechanism. For a Gaussian spectral distribution, the respective weights μ_i of the viscous mechanism are defined by:

$$\mu_i = \frac{1}{n_0 \sqrt{\pi}} \times \exp\left(-\left(\frac{n_i - n_c}{n_0}\right)^2\right) \quad (5)$$

with $n_i = n_c - n_0 + (i-1)\Delta$: i^{th} relaxation mechanism, $\Delta = \frac{2n_0}{n_b - 1}$ is time interval between two relaxation

times, n_b is total number of mechanisms ($n=30$), n_0 is its standard deviation and n_c is its average. From a physical point of view, n_0 gives an enhanced effect on late mechanisms and increase of n_c tends to homogenize the weights. The distribution of the relaxation mechanisms' weight is normalized such as:

$$\sum_{i=1}^{n_b} \mu_i = 1 \quad (6)$$

The viscoplastic behavior is activated only when the stress exceeds the yield strength $\tau_y(T)$, which is assumed to be the same for plasticity and viscoplasticity in PMCs. In addition, the elastic and viscoplastic behaviors are supposed to be independent of each other for the considered loading rates, and the restoring phenomena is negligible.

$$f_{vp}(\underline{\sigma}, \underline{X}) = \overline{(\underline{\sigma} - \underline{X})} - \tau_y(T) \quad (7)$$

where $\overline{(\underline{\sigma} - \underline{X})} = \sqrt{\underline{(\underline{\sigma} - \underline{X})} : \underline{\underline{M}} : (\underline{\sigma} - \underline{X})}$ is the equivalent constraint, $\underline{\underline{M}}$ is a fourth order tensor describing the anisotropy of viscoplastic flow in shear loading

$$\underline{\underline{M}} = \begin{pmatrix} 0 & 0 & 0 & 0 & 0 & 0 \\ 0 & 0 & 0 & 0 & 0 & 0 \\ 0 & 0 & 0 & 0 & 0 & 0 \\ 0 & 0 & 0 & 1 & 0 & 0 \\ 0 & 0 & 0 & 0 & 0 & 0 \\ 0 & 0 & 0 & 0 & 0 & 1 \end{pmatrix} \quad (8)$$

In the case of a linear kinematic hardening, the thermodynamic force \underline{X} associated with the kinematic hardening variable $\underline{\alpha}$ is defined by:

$$\underline{X} = \delta \underline{\alpha} \quad (9)$$

where δ is a material parameter. The laws of behavior are derived from a thermodynamic potential such as:

$$\dot{\underline{\epsilon}}^{vp} = K \langle f_{vp} \rangle^N \frac{\partial f}{\partial \underline{\sigma}} \quad \text{and} \quad \dot{\underline{\alpha}} = -K \langle f_{vp} \rangle^N \frac{\partial f_{vp}}{\partial \underline{X}} \quad (10)$$

with N is a parameter representing the material rate sensitivity and K is a parameter seen as a penalty coefficient. The classical time-independent plasticity expression is recovered when $K \rightarrow \infty$. With respect to the viscoplastic yield function f , those laws can be written as

$$\dot{\underline{\epsilon}}^{vp} = \dot{\lambda}_{vp} \frac{\underline{\underline{M}}(\underline{\sigma} - \underline{X})}{(\underline{\sigma} - \underline{X})} \quad \text{and} \quad \dot{\underline{\alpha}} = \dot{\lambda}_{vp} \frac{\underline{\underline{M}}(\underline{\sigma} - \underline{X})}{(\underline{\sigma} - \underline{X})} = \dot{\underline{\epsilon}}^{vp} \quad (11)$$

where $\dot{\lambda}_{vp} = \sqrt{\underline{\underline{M}} : \dot{\underline{\epsilon}}^{vp} : \underline{\underline{M}}}$ is the Lagrange viscoplastic multiplier homogeneous to a strain rate. The interpretation of the rate-dependent phenomenon as a penalty regularization of the rate-independent one is applied. Thus, the concept of "dynamic" yield function allows us to use the postulate of maximum dissipation in a straightforward manner, and to derive the "static" yield function in a consistent manner.

$$f_{vp}^{dyn}(\underline{\sigma}, \underline{X}, \dot{\lambda}_{vp}) = f_{vp}(\underline{\sigma}, \underline{X}) - (\dot{\lambda}_{vp} / K)^{\frac{1}{N}} \quad (12)$$

The viscoplastic model was implemented in the code finite element software Cast3M.

IV. SIMULATIONS AND ANALYSIS

IV.1. Numerical simulation of the tensile test

The overall behavior of the laminates in terms of stress-strain response (Fig. 3a). The first, we can observe the evolution elastic-viscoelastic deformation. In this phase, the result of the simulation is almost identical to the experimental one. In the viscoplastic phase, we can observe the evolution of the distribution of the cumulated plastic deformation. These distributions confirm the viscoplastic character of the resin since the cumulated plastic deformation, which is maximum at the right edge of the hole [20,21].

The comparison of the experimental and numerical response shows that the developed numerical model allows to correctly reproduce the mechanical behavior of perforated laminates with plies oriented at 45° for the direction of the load. In the configuration [±45]₇, the response of the laminate is mainly governed by the behavior of the matrix. In other term, the viscoplastic behavior of the resin is well taken into account by the model.

IV.2. Numerical simulation of the load/unload test

In some early cycles, the results of the experiment and simulation are almost identical. It is important to note that the loading rate remains the same for each loading-unloading, but then (after 25 cycles) the deformation of simulation is greater than experiment, while the value of the stress is the same (142.31 MPa for simulation and 142.88 MPa for experiment) (Fig. 3b).

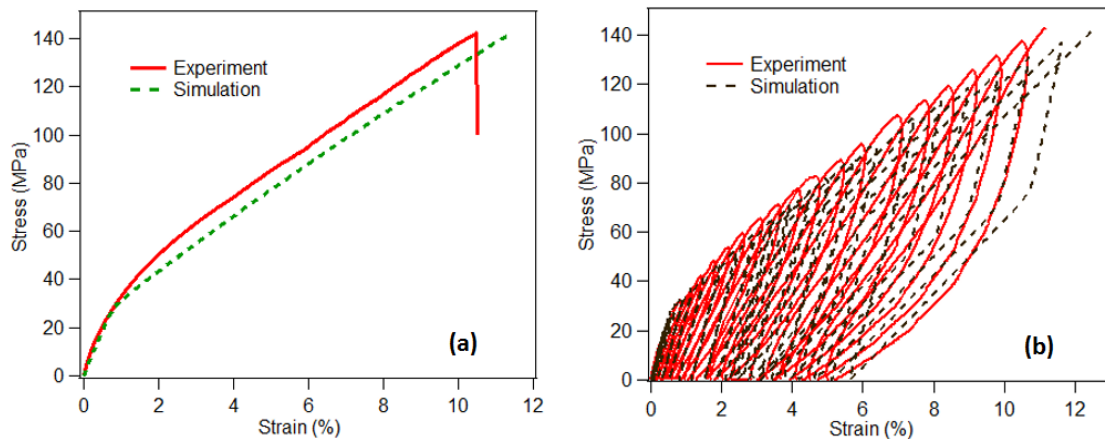


Fig. 3. Comparison of mechanical responses between experiment and simulation:
(a) Tensile test, (b) Load/Unload test

The difference is due: In the experiment, all mechanisms of late damage are also dependent on time and collaborate with polymer creep. The viscoelastic - viscoplastic behavior change in each cycle, especially the decrease in the rigidity of laminates is different. On the other hand, the very ductile behavior of the CPPS at $T > T_g$ leading to the evaluation of rigidity becomes difficult, therefore after each cycle the increment of deformation is different. For simulation, after each cycle, the strain increment is constant.

IV.3. Numerical simulation of fatigue loading test

Fig. 4 shows that there is little difference between experiment and simulation. In the stable state, the stress and strain values are different but it is acceptable. At the end of each cycle, the stress value is equal to zero for simulation but for the experiment, it is not equal zero. This difference can be explained as follows: in the experiment, the rate of displacement on the specimen test is less than the loading rate of the machine for each loading-unloading, thus the waveform shape appears on the stress - strain curves.

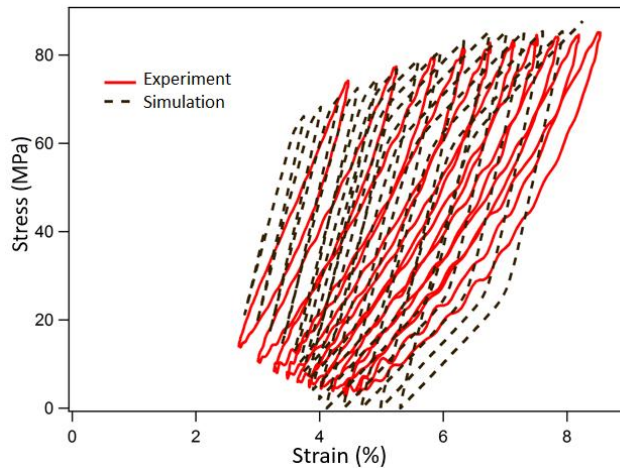


Fig. 4. Experimental vs simulation fatigue loading responses

IV.4. Comparison between plastic model and viscoplastic model with experiment

The stress concentrator is very important in engineering design because it is directly related to the strength of the structure. The tracing of the longitudinal overstress profiles to the right edge of the hole is necessary in view of the application for early design stage. It allows knowing the evolution of the overstress coefficient K_t in function of the distance to the edge of the hole. The K_t is defined by the ratio of the maximum overstress near the hole and the stress applied at the specimen's ends [20,21]. For the two models studied in this section, we can observe the differences in maximum overstress in the plastic-viscoplastic phase (Fig. 5).

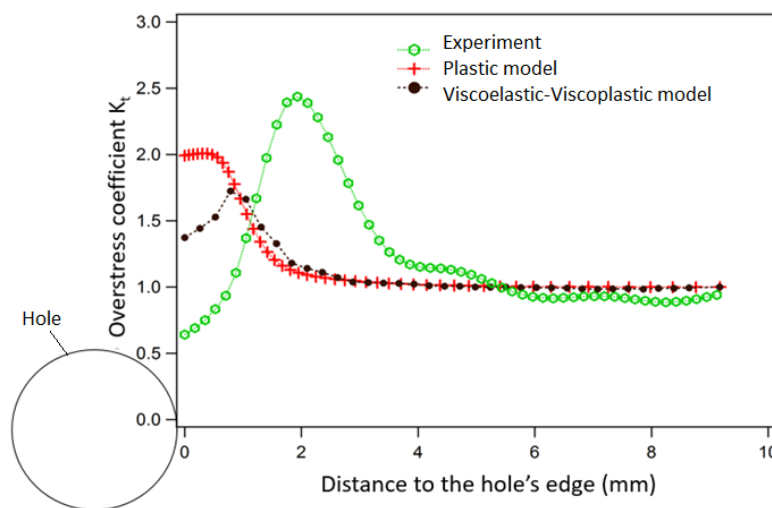


Fig. 5. Comparison of experimental and numerical overstress profiles in notched C/PPS laminates

From the over stresses accommodation standpoint, in the fiber bundles near the hole, plasticity is too limited to relax the stresses. Therefore, with the same hole factor C_h , the over stresses value in the viscoplastic model less than in the plastic mode. The comparison of the experimental over stresses profiles at before failure with simulation show that K_t increases at 120°C near the hole in simulation. In AP laminates, the mechanical behavior is mainly matrix dominated [22]. It has an impact on stresses distribution around the hole through a plasticity mechanism. However, it is not only mechanism for accommodating over stresses but also depends on temperature test and structure of specimens [20,21]. Based on the conclusions done in previous studies of over stress accommodation in notched C/TP composite laminate and numerical tool standpoint, we noticed that the rotation of fibers is not taken into account for numerical plastic models. The observation of fibers at the surface of failed specimens show that such a rotation of fiber bundles does not occur, and there is no observable necking [22]. For viscoplastic model, the rotation of fibers bundles is taken into account, but it probably would not improve that much the predictive capabilities of the model [18]. The deviations between simulation and experiment shown that the damage near the hole has an important role. For thermomechanical behavior of angle-ply laminates, it should be considered into the model formulation to account more accurately for the over stress accommodation.

V. CONCLUSION

In this study, we have proposed a code finite element to implement in the software Cast3M. This code allows us to predict the mechanical behavior of the specimens without carrying out the experiments. It is also used to simulate the overstress profiles near the hole. The numerical results obtained are in good agreement with the experimental results. Besides, we have shown that viscoelastic - viscoplastic model should be considered into the model formulation to account more accurately for the overstress accommodation.

REFERENCES

- [1]. Harris B. Science and technology of the fatigue response of fiber-reinforced plastics: Woodhead, Cambridge. 2003, Fatigue in composites.
- [2]. Kawai M, Masuko Y. Macromechanical modeling and analysis of the viscoplastic behavior of unidirectional fiber-reinforced composites. *J Compos Mater*, 2003; 37(21), pp. 1885–1902.
- [3]. Muliana AH, Kim JS. A concurrent micromechanical model for predicting nonlinear viscoelastic responses of composites reinforced with solid spherical particles. *Inter J Solid Struct* 2007;44(21):6891–913
- [4]. Harris JS, Barbero EJ. Prediction of creep properties of laminated composites from matrix creep data. *J ReinfPlast Compos* 1998;17(4), pp. 361–379.
- [5]. Lahellec NI, Suquet P. Effective behavior of linear viscoelastic composites: a time-integration approach. *Inter J Solids Struct* 2007;44(2), pp. 507–529.
- [6]. Hashin Z. Complex moduli of viscoelastic composites I. General theory and application to particulate composites. *Int J Solids Struct* 1970; 6(5), pp. 539–552.
- [7]. Schapery RA. Nonlinear viscoelastic and viscoplastic constitutive equations based on thermodynamics. *Mech Time-Depend Mater* 1997; 1(2), pp. 209–240.
- [8]. Nordin L-O, Varna J. Nonlinear viscoplastic and nonlinear viscoelastic material model for paper fiber composites in compression. *Composites Part A* 2006; 37(2), pp. 344–355.
- [9]. Al-Haik MS, Hussaini MY, Garmestani H. Prediction of nonlinear viscoelastic behavior of polymeric composites using an artificial neural network. *Inter J Plast* 2006; 22(7), pp. 1367–1392.
- [10]. Ha SK, Wang Q, Chang F-K. Modeling the viscoplastic behavior of fiber-reinforced thermoplastic matrix composites at elevated temperatures. *J Compos Mater* 1991; 25, pp. 334–372.
- [11]. Kawai M, Masuko Y, Kawase Y, Negishi R. Micromechanical analysis of the off-axis rate-dependent inelastic behavior of unidirectional AS4/PEEK at high temperature. *Inter J Mech Sci* 2001; 43(9), pp. 2069–2090.
- [12]. Masuko Y, Kawai M. Application of a phenomenological viscoplasticity model to the stress relaxation behavior of unidirectional and angle-ply CFRP laminates at high temperature. *Composites Part A* 2004;35(7–8), pp. 817–826.
- [13]. Gates TS, Sun CT. Elastic/viscoplastic constitutive model for fiber reinforced thermoplastic composites. *AIAA J* 1991; 29(3), pp. 457–463.
- [14]. Weeks CA, Sun CT. Modeling non-linear rate-dependent behavior in fiber-reinforced composites. *Compos Sci Technol* 1998; 58(34), pp 603–611.
- [15]. Ding SR, Huo YZ, Tong JW, Shen M, Aymerich F, Priolo P. Viscoplastic analysis of the off-axis rate-dependent inelastic behavior of unidirectional AS4/PEEK. *J ReinfPlast Compos* 2006; 25(5), pp. 475–482.
- [16]. Chen JL, Sun CT. Modeling creep behavior of fiber composites. In: *Proceedings of the American Society for Composites, Third technical Conference* 1988, 11.
- [17]. Zhang Z, Friedrich K. Artificial neural networks applied to polymer composites: a review. *Compos Sci Technol* 2003;63(14), pp 2029–2044.
- [18]. W. Albouy, B. Vieille, L. Taleb. Experimental and numerical investigations on the time-dependent behavior of woven-ply PPS thermoplastic laminates at temperatures higher than glass transition temperature. *Composites: Part A* 2013, 49, pp. 165–178.
- [19]. Boubakar ML, Vang L, Trivaudey F, Perreux D. A meso-macro finite element modelling of laminate structures: Part II: time-dependent behavior. *Compos Struct* 2003;60(3), pp 275–305.
- [20]. B. Vieille, J. Aucher, L. Taleb. Overstress accommodation in notched woven-ply thermoplastic laminates at high temperature: Numerical modeling and validation by Digital Image Correlation. *Composites Part B* 2013, 45, pp. 290-302
- [21]. B. Vieille, L. Taleb. About the influence of temperature and matrix ductility on the behavior of carbon woven-ply PPS or epoxy laminates: Notched and unnotched laminates. *Composites Science and Technology* 2011, 71, pp. 998-1007.
- [22]. Luong Viet Dung and Duong Pham Tuong Minh, Fatigue mechanical behavior at high temperature of Carbon/Polyphenylene Sulfide Composite laminates, *Journal of Science & Technology* 2016, 112, pp. 054-059.